JOURNAL OF MATERIALS SCIENCE 37 (2002) 2273–2278

# Microstructure, mechanical properties and ionic conductivity of BICUVOX - $ZrO_2$ composite solid electrolytes

M. H. PAYDAR, A. M. HADIAN
*Department of Metallurgy and Materials, Faculty of Engineering, University of Tehran, Tehran, Iran*

K. SHIMANOE, N. YAMAZOE
*Department of Materials Science, Faculty of Engineering Sciences, Kyushu University, Kasuga-shi, Fukuoka 816-8580, Japan*
*E-mail: yamazoe@mm.kyushu-u.ac.jp*

The composites of Cu-partially substituted bismuth vanadate (BICUVOX.1) mixed with a small amount of partially stabilized zirconia (3Y-TZP) were prepared to investigate their microstructure, mechanical properties and ionic conductivity. It was found that the addition of 0.5 to 1 wt% 3Y-TZP reduces the grain size to lower than 1 $\mu$m in diameter, leading to improvements in micro-hardness and toughness by more than 15%. Due to preferential distribution of 3Y-TZP particles along grain boundaries, grain boundary conductivity and total conductivity decreased with increasing 3Y-TZP content at low temperature, but the decrements remained rather modest and, in addition, became less significant at higher temperature to disappear at 700 K and above. 

## 1. Introduction

A bismuth vanadate with Bi/V = 2 in atomic ratio, $Bi_4V_2O_{11}$ or $Bi_2VO_{5.5}$, was first synthesized by Bush *et al*. [1], and its exiting properties were discovered by Abraham *et al*. [2]. The compound has a layered structure in which the layers of $(Bi_2O_2)^{2+}$ and $(VO_{3.5}\square_{0.5})^{2-}$ are stacked alternately. The oxygen vacancies ($\square$) are disordered in the high temperature phase ($\gamma$) of the compound, providing the phase with a high oxide ionic conductivity. The disordered phase close to $\gamma$ can be stabilized effectively down to room temperature by partial substitution of other metals (Me) for V. The family of partially substituted compounds, $Bi_2V_{1-x}Me_xO_{5.5-3x/2}$, have thus been derived, where Me = Cu, Ni, Co, Ti, etc., and $x$ is the molar substitution of the metal cation selected for vanadium. These compounds are designated by the acronym BIMEVOX, and, if necessary, the molar substitution of Me($x$) is indicated by attaching $x$ to the acronym like BIMEVOX.1 according to the proposal of the frontier group [3]. With their excellence in oxide-ionic conductivity and electrocatalytic activity, BIMEVOX materials have turned out to be very promising for application to electrochemical devices such as one for the separation of oxygen from air. A considerable number of studies have been carried out on the crystal structures, ionic conductive and electrocatalytic properties [3–10] of BIMEVOX materials. However, the mechanical properties of the materials have been hardly investigated well, in spite of their importance in the application for devices.

On this background, we started mechanical properties-related studies on the 0.1 molar Cu-substituted material (BICUVOX.1), the most important one of the family. It was found that the material tends to undergo unusual grain growth in the sintering process and that the addition of zirconia by a small amount effectively suppresses the growth, leading to significant improvements in the mechanical properties. This paper aims at describing how the addition of zirconia affects the microstructure, mechanical properties (toughness and hardness), and ionic conductivity of BICUVOX.1 material.

## 2. Experimental procedure

The powder of BICUVOX.1, i.e., $Bi_2Cu_{0.1}V_{0.9}O_{5.35}$, was prepared from a stoichiometric mixture of the constituent metal oxides of analytical grade (Aldrich, 99.99% purity) by a solid-state reaction method. The mixture suspended in ethanol was ground in an attrition mill with zirconia balls (3 mm in diameter) for 5 h, and, after drying, calcined in air at 650°C for 15 h. The mixture was ground again in the same way as before and recalcined at 750°C for 5 h. The resulting powder was further subjected to the grinding for about 20 h to reduce the particle size to less than 1 $\mu$m in diameter. When necessary, this powder was loaded with (0.5 or 1.0 wt%) of 3-mol% $Y_2O_3$ stabilized $ZrO_2$ (3Y-TZP) (Tosoh, Japan). For this purpose, the weighed amounts 3Y-TZP powder was dispersed in ethanol under ultrasonic vibration before it was mixed with BICUVOX.1

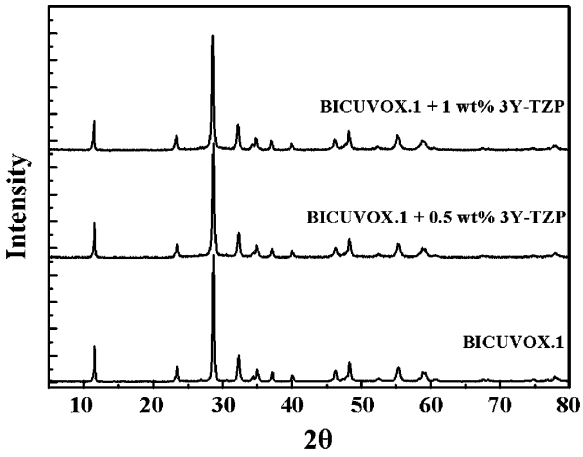


*Figure 1* XRD pattern of BICUVOX.1 and BICUVOX.1 + 3Y-TZP composite samples.

powder by using the attrition mill zirconia balls for 30 h, followed by drying. Each BICUVOX.1 powder, loaded with or without 3Y-TZP, was compacted into a disc specimen, 10 mm in diameter and 1.5 mm thick, or a rod specimen of $3 \times 4 \times 33$ mm in size under hydrostatic pressure at 350 MPa. The green body obtained was sintered at temperature ranging from 730 to 750°C for 5 to 10 h, because these conditions were optimum for sintering as found in the pervious work [11].

The disc specimen was used for investigating the microstructure and ionic conductivity. For the microscopic observation, the specimen was polished with a fine diamond paste (diamond grain of 0.5 $\mu$m in diameter) and then thermally etched at 650°C for 2 h. The resulting surface was observed on a field emission type scanning electron microscope (FE-SEM, JEOL JSM-6340GF). For the ionic conductivity measurements, both sides of the disc specimen were polished with SiC sand papers (up to grade 2000), and then attached with Pt electrodes by applying a Pt paste followed by firing at 30°C for 3 h in air. Electrical contacts were made by pressing spring-loaded Pt wire-Pt mesh attachments against the painted electrodes. The measurements were performed in the temperature range of 100 to 700°C in the flow of artificial air by utilizing an ac two-probe impedance spectrometer (Model 1260, Solartron, Hampshire, U.K.) apparatus in the frequency range of 1 to 10 MHz. The real and imaginary components of the impedance over the frequency range were plotted on the complex plane to determine the bulk and grain boundary resistances based on the equivalent circuit model introduced by Dygas *et al*. [12], as a modification of Bauerle's model [13]. The circuit parameters were estimated by using a nonlinear least-square fitting with the aid of Zplot software (Scribner Associates, Inc., U.S.A).

The rod specimen was used for investigating microhardness and fracture toughness by means of the Vickers test method (Akashi, AVK-C1) and the three-points bending test method using notched samples as specified by Japanese Industrial Standard (JIS) Z 8401, respectively. The latter test was carried out by using a bending jig with a span of 16 mm and a cross head speed of 0.5 mm/min. All the rod specimens were polished with a diamond paste before the mechanical tests.

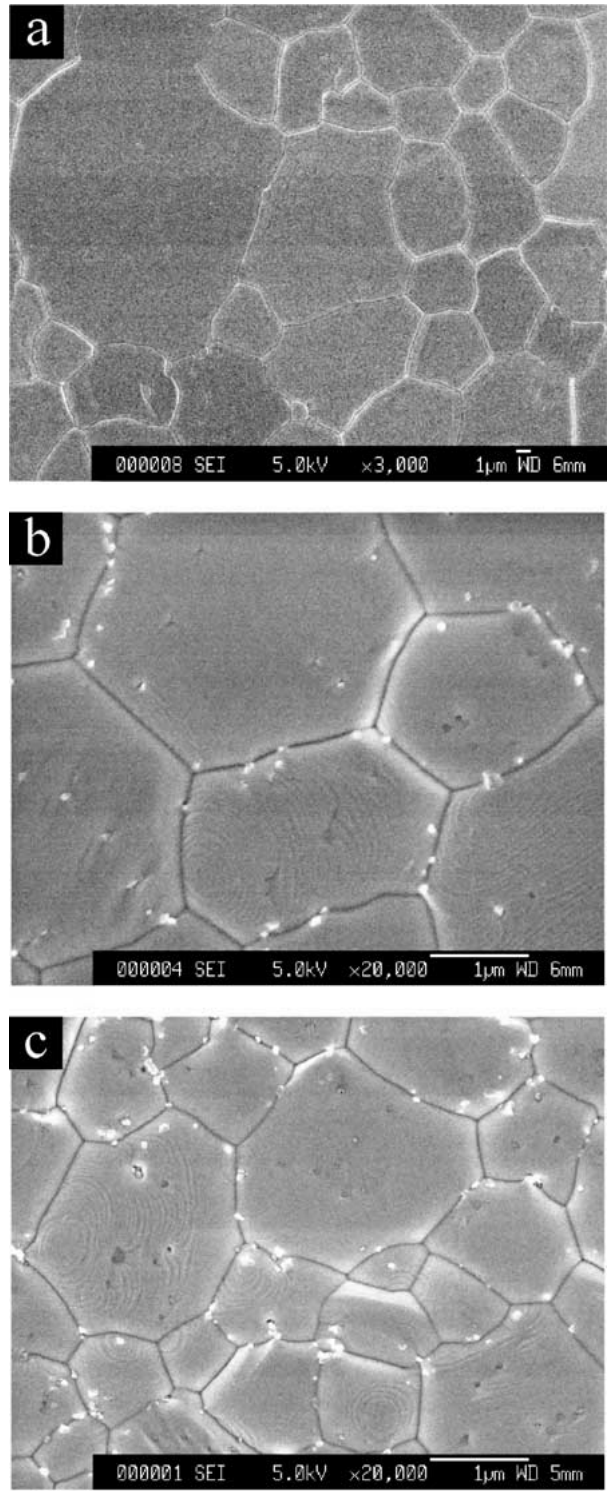


*Figure 2* Micrographs of (a) BICUVOX.1, (b) BICUVOX.1 + 0.5 wt% 3Y-TZP and (c) BICUVOX.1 + 1 wt% 3Y-TZP samples sintered at 1003 K for 10 h.

## 3. Results and discussion

### 3.1. Microstructural characterization

The XRD patterns (Cu $K_\alpha$ radiation) of the BICUVOX.1 powder samples containing 0, 0.5 and 1 wt% 3Y-TZP after calcination at 750°C for 5 h are shown in Fig. 1. All of these patterns are coincident with that of $\gamma$-$Bi_4V_2O_{11}$ parent phase [1, 2]. This suggests that the 3Y-TZP component added is not incorporated in the crystal lattice of BICUVOX.1 but is present outside of the BICUVOX.1 matrix. This suggestion was supported from the SEM images of the surfaces of sintered

disc specimens shown in Fig. 2. Owing to the attrition milling for about 20 h, the BICUVOX.1 compound had been pulverized into a fine powder with a small particle size less than 0.5 $\mu$m, which was beneficial to the sintering processes of the green compacts. As the micrographs indicate, all the specimens after sintering had microstructure consisting of closely packed grains, the relative density of which exceeded 95% of the theoretical value [11]. For the pure BICUVOX.1 specimen, most of grains had sizes far exceeding a few $\mu$m, resulting in a wide grain size distribution. The addition of 3Y-TZP decreased the grain size drastically, as clearly seen from the images. As a result of this effect, the average grain sizes were 10, 2.5 and 1 $\mu$m for the specimens containing 0, 0.5 and 1 wt% 3Y-TZP, respectively. A striking feature was that the submicron particles of 3Y-TZP, seen as bright spots, distributed preferentially along the boundaries of BICUVOX.1 grains. It is considered that 3Y-TZP particles were excluded from the BICUVOX.1 grains during the grain growth processes, being segregated along the grain boundaries. This segregation seemed to suppress the further growth of grains.

## 3.2. Mechanical properties

Fig. 3 shows the micro-hardness ($H_v$) and fracture toughness ($K_{Ic}$) of the BICUVOX.1–based rod specimens as a function of zirconia content. Both $H_v$ and $K_{Ic}$ increased with increasing 3Y-TZP content, being improved by 21 and 18.2% at the 1 wt% 3Y-TZP content, respectively. These improvements can be attributed to the reduction of the grain size or the increase of the grain boundary density just mentioned. The improvement in $K_{Ic}$ is understood intutionally as resulting from the deflection of microcracks at the grain boundaries [14, 15]. It is known that the microcracks formed in the specimen are deflected along the grain boundaries and this decreases the average stress normal to the crack plane at its tip. With reducing the grain size, the number of crack deflection increases, increasing fracture toughness ($K_{Ic}$). A similar phenomenon has been reported for a nanocomposites solid electrolyte of 8YSZ/SiC [16]. More quantitatively, fracture toughness is usually proportional on the fracture strength ($\sigma_f$) which is well

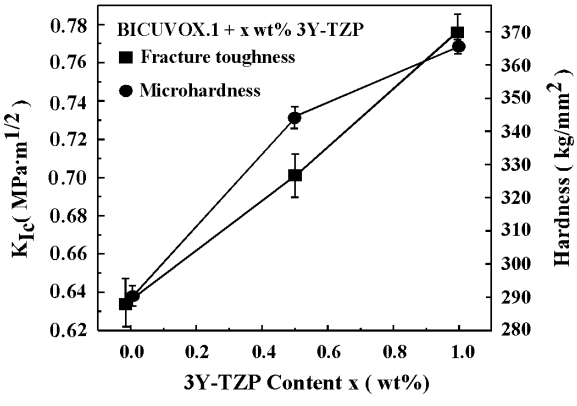


*Figure 3* Microhardness and fracture toughness of BICUVOX.1 on the dependence of addition of 3Y-TZP.

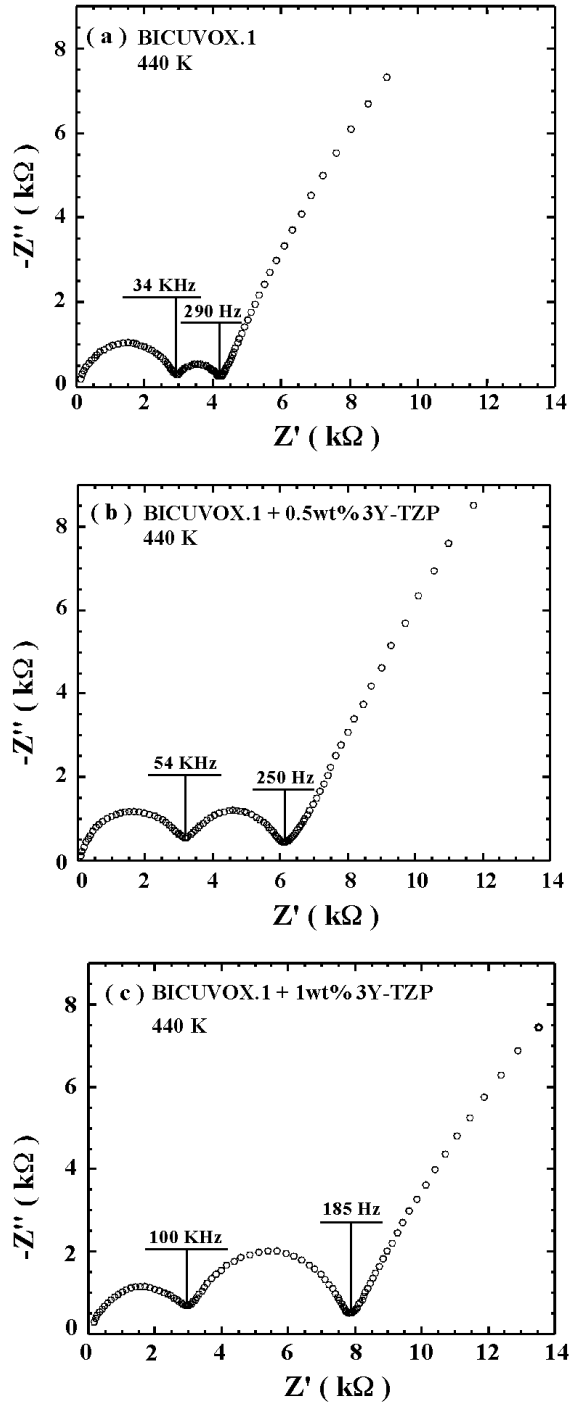


*Figure 4* Impedance spectra of BICUVOX.1 and BICUVOX.1 + 0.5 and 1wt% 3Y-TZP at 440 K.

correlated with the grain size by the following equation:

$$\sigma_f = \sigma_o + Kd^{-1/2} \quad (1)$$

where $\sigma_o$ is characterstic strength, $k$ a constant, and $d$ the grain size. Micro-hardness ($H_v$) is also correlated with the grain size through $\sigma_f$ as follows:

$$H_v = n \cdot \sigma_f \quad (2)$$

where $n$ is a constant in the range of 20 to 50. These equations show $H_v$ and $K_{Ic}$ increase as $d$ decreases.

### 3.3. Ionic conductivity characterization

Impedance measurements were carried out for the BICUVOX.1 based disc specimens containing 0, 0.5 and 1 wt% 3Y-TZP at 440 K. The specimens were controlled to have the same geometrical factor, i.e., $S/d = 2.6$ cm, where $S$ is the area of the deposited electrodes, and $d$ is the distance between electrodes. The resulting Nyquist plots are shown in Fig. 4. Each spectrum followed well the Bauerle [13, 17] type behavior, characterized by the two semicircles attributed to the contributions of the bulk and the grain boundaries to the total ionic impedance, respectively, prior to the monotonic ascent due to electrode reactions. The first semicircles (bulk contribution) remained essentially the same for these specimens. The second semicircles (grain boundary contribution) obviously enlarged with increasing 3Y-TZP content from 0 (Fig. 4a) through 1 wt% (Fig. 4c). This tendency coincides well with the microscopic observation that the grain size of BICUVOX.1 decreased, or the grain boundary density increased, with increasing 3Y-TZP content.

The bulk resistance ($R_b$) and grain boundary resistance ($R_{g.b}$), which are given from the $Z'$ values at the minimum points in each spectrum, were determined by simulating each spectrum based on the equivalent circuit model introduced by Dygas [12]. The resistance values thus determined were transformed into the bulk conductivity ($\sigma_b$), grain boundary conductivity ($\sigma_{g.b}$), and total conductivity ($\sigma_t$) by using the following equation:

$$\sigma = (1/R)(d/S) \tag{3}$$

where $R$ is the resistance of the bulk or grain-boundaries.

The same impedance measurements were carried out over the temperature range between 100 and 700°C. Fig. 5 shows the log ($\sigma$.T) values for the bulk, grain boundary, and total conductivities, respectively, as a function of reciprocal temperature. From these correlations, activation energy ($E_a$) of each conductivity was estimated by assuming the following Arrhenius equation:

$$\sigma = (\sigma_o/T)\exp(-E_a/kT) \tag{4}$$

Here $\sigma_o$ is a preexponential constant, $T$ the temperature ($K$), $E_a$ the activation energy (eV), and $k$ the Boltzmann constant. The activation energy data thus estimated as well as the conductivity data at 473, 673 and 873 K are listed for the three specimens in Table I.

It is possible to point out a few important facts from the above data. First of all, the three specimens exhibited essentially the same bulk ionic conductivity ($\sigma_b$) at fixed temperature regardless the differences in 3Y-TZP content (Fig. 5a). This is quite natural if one considers that 3Y-TZP particles are excluded from the grains of BICUVOX.1. The log ($\sigma.T$) versus $1000/T$ correlation had an inflection at a temperature between 700 and 750 K, indicating a change in activation energy. It is well known that the BIMEVOX materials transform from $\gamma'$ phase to $\gamma$ in this temperature range on heating. The decrease of activation energy from 0.7 eV

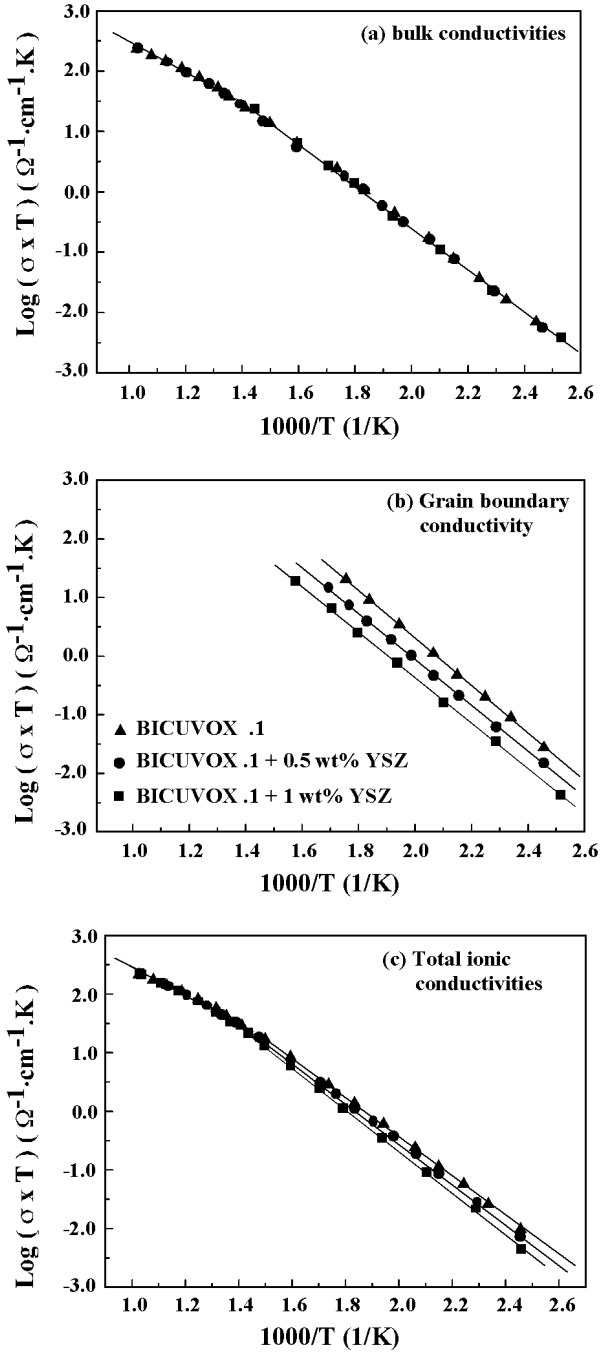


*Figure 5* Arrhenius plots of (a) Bulk, (b) Grain boundary and (c) Total ionic conductivity for BICUVOX.1 and BICUVOX.1 + 3Y-TZP.

($T < 700$ K) to 0.45 eV ($T > 800$ K) reflects well that $\gamma$ phase has higher degree of disordering of oxygen vacancies than $\gamma'$. The grain boundary conductivity ($\sigma_{g.b}$), on the other hand, decreased significantly with increasing 3Y-TZP content in the temperature range below 650 K (Fig. 5b). This tendency is also natural because the density of grain boundaries increases with increasing 3Y-TZP content. It is also possible that the inclusion of 3Y-TZP particles in each grain boundary increases, leading to a decrease in $\sigma_{g.b}$, but the contribution of this effect is considered to be minor in the present study. It should be remarked that the grain boundary conductivity (or resistance) could not be measured at the higher temperature above 650 K, because the corresponding second semicircles in the impedance spectra became smaller as temperature increased, and

TABLE I Conductivities and activation energies for BICUVOX.1-based composites

| Sample type | Conductivity × $10^3$ ($\Omega^{-1} \cdot cm^{-1} \cdot K$) | | | Activation energy (eV) | |
|---|---|---|---|---|---|
| | 473 K | 673 K | 873 K | $T < 720$ K | $T > 780$ K |
| BICUVOX.1 | | | | | |
| Bulk | 0.465 | *29.2 | *154 | 0.65 | 0.4 |
| Grain boundary | 1.25 | – | – | 0.78 | – |
| Total conductivity | 0.315 | 29.2 | 154 | 0.675 | 0.4 |
| BICUVOX.1 + 0.5 wt% 3Y-TZP | | | | | |
| Bulk | 0.435 | *25.5 | *148 | 0.645 | 0.46 |
| Grain boundary | 0.623 | – | – | 0.77 | – |
| Total | 0.26 | 25.5 | 148 | 0.694 | 0.46 |
| BICUVOX.1 + 1 wt% 3Y-TZP | | | | | |
| Bulk | 0.456 | *22 | *150 | 0.645 | 0.46 |
| Grain boundary | 0.324 | – | – | 0.78 | – |
| Total | 0.18 | 22 | 150 | 0.71 | 0.46 |
| BICUVOX.1 | | | | | |
| Total conductivity | | | | | |
| Ref. [4] | 0.4 | 19.6 | 113 | 0.6 | |
| Ref. [12] | 0.12 | 11.4 | – | 0.666 | |

The mark (*) shows that the value is the same as total conductivity.

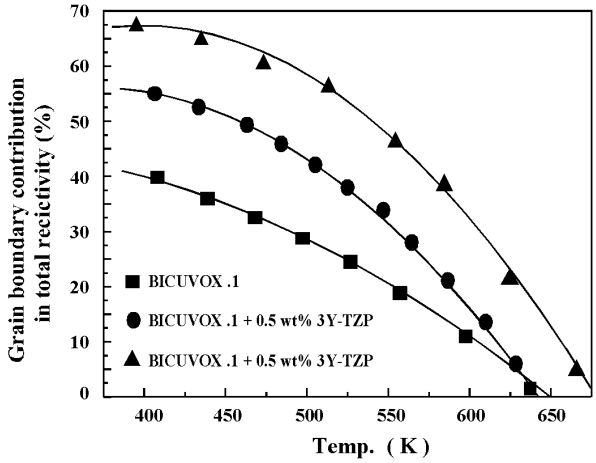


*Figure 6* Grain boundary contribution in total resistivity.

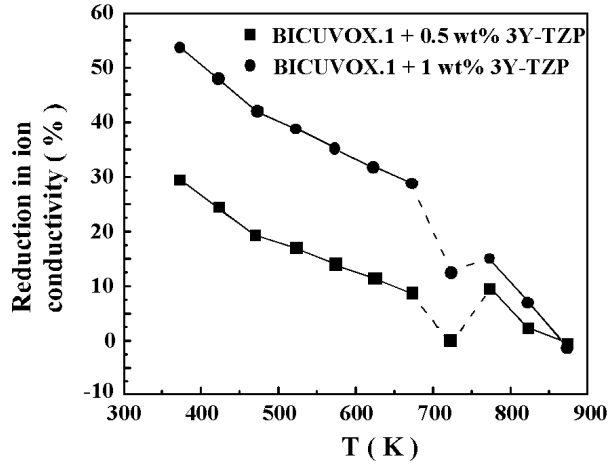


*Figure 7* Reduction in ion conductivity of BICUVOX.1 + 3Y-TZP as a function of temperature.

disappeared completely at that temperature and above. Reflecting such behavior of $\sigma_b$ and $\sigma_{g.b}$, the total ionic conductivity ($\sigma_t$) decreased slightly with increasing 3Y-TZP content in the temperature range up to 700 K, while it coincided with the bulk conductivity above 700 K. The total conductivity estimated here was fairly close to that reported recently [4, 12], as seen from Table I.

As stated above, the addition of 3Y-TZP reduces the grain boundary conductivity ($\sigma_{g.b}$) only, leaving the bulk conductivity ($\sigma_b$) intact. The effects of 3Y-TZP addition can be illustrated more clearly in terms of the grain boundary resistance ($R_{g.b}$). Fig. 6 shows the $R_{g.b}$ values normalized by the total resistance ($R_t = R_{g.b} + R_b$) as a function of temperature for the three specimens. In the pure BICUVOX.1 specimen, $R_{g.b}$ shared about 40% of $R_t$ at 400 K and decreased with increasing temperature, disappearing at about 650 K. The addition of 3Y-TZP tended to shift the correlations upward, but the shifts were not so large and, in ddition, $R_{g.b}$ totally disappeared at 700 K even for the specimen added with 1 wt% 3Y-TZP.

The effects of 3Y-TZP addition on the total conductivity ($\sigma_t$) are shown in Fig. 7, where the percentage of reduction in $\sigma_t$ with the addition of 0.5 or 1 wt% 3Y-TZP to BICUVOX.1 is shown as a function of temperature. The reduction was more conspicuous with increasing 3Y-TZP content, but it went down rather sharply toward zero with increasing temperature. The correlation lines showed discontinuities in the temperature range of 720–770 K due to the $\gamma' \rightarrow \gamma$ phase transformation already stated.

## 4. Conclusion

The addition of 3Y-TZP (0.5 or 1 wt%) can improve the mechanical properties of BICUVOX.1 ceramic without degrading its oxide-ionic conductivity seriously. The particles of 3Y-TZP added are distributed along the grain boundaries of BICUVOX.1, executing an intense effect to reduce the grain size. Through this effect, the micro-hardness and fracture toughness of the ceramic can be improved by more than 15% with the addition of 1 wt% 3Y-TZP. Inclusion of 3Y-TZP particles in the grain boundaries leads to decreases in grain boundary conductivity and total conductivity especially at lower temperature, but the decreases remain rather moderate and become less significant at higher temperature. These results assure that the BICUVOX.1–3Y-TZP composites serve as oxide-ion conducting solid electrolytes with improved mechanical properties.

## Acknowledgement

The authors would like to express their thanks to Prof. H. Abe, Prof. H. Nakashima, Dr. F. Yoshia, and Mr. H. Kitahara for their assistance in measuring the mechanical properties.

## References

1. A. A. BUSH, V. G. KOSHELAYEVA and YU. N. VENEVTSEV, *Jpn. J. Appl. Phys*. **24** (1985) 625.
2. F. ABRAHAM, M. F. DEBREUILLE-GRESSE, G. MAIRESSE and G. NOWOGROCKI, *Solid State Ionics* **28–30** (1988) 529.
3. F. ABRAHAM, J. C. BOIVIN, G. MAIRESSE and G. NOWOGROCKI, *ibid*. **40/41** (1990) 934.
4. S. P. SIMNER, D. SUAREZ-SANDOVAL, J. D. MACKENZIE and B. DUNN, *J. Amer. Ceram. Soc*. **80** (1997) 2563.
5. F. KROK, W. BOGUSZ, P. KUREK, M. WASIUCIONEK, W. JAKUBOWSKI and J. R. DYGAS, *Mater. Sci. Eng*. B**21** (1993) 70.
6. J. R. DYGAS, P. KUREK and M. W. BREITER, *Electrochim. Acta* **40** (1995) 1545.
7. M. C. STEIL, J. FOULETIER, M. KLEITZ and P. LABRUNE, *J. Europ. Ceram. Soc*. **19** (1999) 815.
8. E. PERNOT, M. ANNE, M. BACMANN, P. STROBEL, J. R. FOULETIER, R. N. VANNIER, G. MAIRESSE, F. ABRAHAM and G. NOWOGROCKI, *Solid State Ionics* **70/71** (1994) 259.
9. J. C. BOIVIN, C. PIROVANO, G. NOWOGOROCKI, G. MAIRESSE, PH. LABRUNE and G. LAGRANGE, *ibid*. **113–115** (1998) 639.
10. G. MAIRESSE, in "t. 2, S'erie *II c*" (C. R. Acad. Sci., Paris, 1999) p. 651.
11. M. H. PAYDAR, A. M. HADIAN, K. SHIMANOE and N. YAMAZOE, *J. Europ. Ceram. Soc.*, in press.
12. J. R. DYGAS, F. KROK, W. BOGUSZ and P. KUREK, *Solid State Ionics* **70/71** (1994) 239.
13. J. E. BAUERLE, *J. Phys. Chem. Solids* **30** (1969) 2657.
14. M. BARSOUM, in "Fundamental of Ceramics" (McGraw-Hill, New York, 1997) p. 415.
15. M. RUHLE and A. G. EVANS, *Prog. Mater. Sci.* **33** (1989) 85.
16. N. BAMBA, Y. H. CHOA, T. SEKINO and K. NIIHARA, *J. Europ. Ceram. Soc.* **18** (1998) 693.
17. N. BONANOS, B. C. STEELE and E. P. BUTLER, in "Impedance Spectroscopy edited by J. R. Macdonald (Wiley, New York, 1987) p. 191.

*Received 29 June*
*and accepted 21 November 2001*